

## Electrical transport in doped multiwalled carbon nanotubes

K. Liu, Ph. Avouris,\* and R. Martel

*IBM Research Division, Thomas J. Watson Research Center, Yorktown Heights, New York 10598*

W. K. Hsu

*School of Chemistry and Environmental Science, University of Sussex, Brighton BN1 9QJ, United Kingdom*

(Received 5 December 2000; published 6 April 2001)

The effects of doping, electron coherence, and electron correlation on the transport properties of boron-doped multiwalled carbon nanotubes are studied. Substitutional boron lowers the Fermi level of the tubes and increases the number of participating conduction channels without introducing strong carrier scattering. From 300 to about 50 K, the tubes show metallic behavior with weak electron-phonon coupling. At lower temperatures the resistance increases, and a zero-bias anomaly is observed. The magnetoresistance is now negative indicating the importance of coherent back-scattering processes. The coherence lengths are measured and dephasing is found to involve weakly inelastic electron-electron collisions. The temperature dependence of the resistance as well as the other low temperature observations can be accounted for by one-dimensional weak-localization theory.

DOI: 10.1103/PhysRevB.63.161404

PACS number(s): 72.15.Rn, 72.15.Qm, 72.20.Fr, 73.23.-b

Carbon nanotubes (CNT's) are low-dimensional materials with fascinating electrical properties. Single shell nanotubes can be metallic or semiconducting depending on their atomic arrangement. While there is a reasonably good agreement between the electronic structure determined by scanning tunneling spectroscopy and single-electron approximation-based calculations,<sup>1-3</sup> low-temperature transport measurements on single-walled nanotubes reveal complex many-body effects.<sup>4-7</sup> Multiwalled nanotubes (MWCNT's) are even more complex systems. In principle, the shells of a MWCNT can have different chiralities. The incommensurate character of the stacking of the different shells and momentum conservation requirements lead to weak coupling between the shells of a MWCNT. As a result, the current at low bias and temperature in a bulk-contacted MWCNT flows only through the outermost shell.<sup>8</sup> With respect to the transport mechanism, some studies have concluded that transport in MWCNT's is ballistic even at room temperature,<sup>9</sup> while others concluded that the transport is Ohmic.<sup>10</sup>

Here we present a study of the transport characteristics of MWCNT's. One important issue involves the role of defects on electrical transport. In particular, substitutional impurities may influence transport through scattering and active doping. For this reason we use MWCNT's substitutionally doped with boron. We also examine the strength of electron-phonon scattering and electron-electron scattering, and evaluate the role of electron coherence and many-body effects on the low-temperature electrical behavior of MWCNT's.

In our study we use four-probe (4P) and 2P resistance and magneto-resistance (MR) measurements covering the temperature range from 300 to 4.2 K. We find evidence of boron-induced multi-mode conduction, and, to the best of our knowledge, for the first time in MWCNT's, a clear metallic region with linear temperature dependence is observed upon cooling. This is followed at lower temperature by the formation of a disorder-induced, weakly localized state (WL). Coherence lengths are extracted from the magneto-resistance (MR) measurements, and weakly inelastic

electron-electron collisions are found to dominate the decoherence mechanism. While a power law can fit the temperature dependence of the conductance, a behavior suggestive of Luttinger liquid formation, coherent back-scattering effects better account for the overall transport behavior.

The B-doped multiwalled carbon nanotubes (B-MWCNT's) were produced by arc discharge between graphite electrodes containing boron.<sup>11</sup> The content of boron in the MWCNT is not very precisely known, but K-edge electron energy-loss spectra indicate a boron content of about 1%. The nanotubes were purified using microfiltration and suspended in 1,2-dichloroethane. This suspension is used to disperse the nanotubes on SiO<sub>2</sub> substrates bearing the 30 nm thick Ti/Au metal electrodes. The electrodes consist of 200 nm wide fingers separated by gaps of 250 nm. This setup allows us to perform both 2P and 4P resistance measurements on single B-MWCNTs. The a.c.(23.3Hz) probe voltage is kept below  $k_B T/e$  over the whole temperature range (4.2 K to 300 K).

Below we present electrical data on two representative B-MWCNT's. Their diameters are 27 nm and 17 nm for samples S1 and S2, respectively. The first important observation is that the low bias conductances of the samples are significantly higher than expected. At room temperature, sample S1 has  $G_{2P}=174 \mu\text{S}$  and  $G_{4P}=443 \mu\text{S}$  while S2 has  $G_{2P}=222 \mu\text{S}$  and  $G_{4P}=500 \mu\text{S}$ . Since a metallic nanotube shell does not have more than two bands crossing at the Fermi energy ( $E_F$ ), the maximum conductance per carbon shell expected at low bias is  $G=2(2e^2/h)=155 \mu\text{S}$ . We have to conclude then that more than two conduction channels contribute to the low bias conductance in the B-MWCNT's. Scanning tunneling microscopy (STM) spectra of the B-MWCNT's on graphite show a lowering of the Fermi level ( $E_F$ ) of the nanotube by  $\leq 0.1$  eV.<sup>12</sup> The energy states (van Hove singularities) of metallic nanotubes with diameters  $D$  are separated by  $3a_0\gamma_0/D$ , where  $a_0$  is the C-C bond length (0.141 nm), and  $\gamma_0$  is the nearest-neighbor C-C interaction energy (2.9 eV). Thus, we find for our

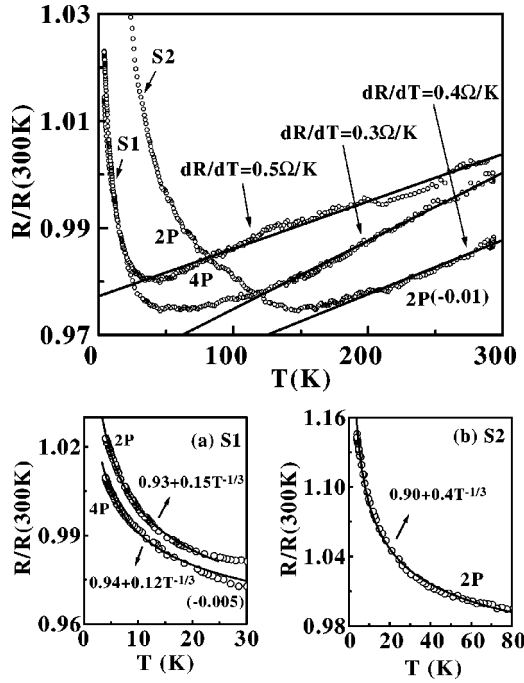


FIG. 1. Top: Temperature dependence of the resistance  $R(T)$  normalized by  $R(300\text{ K})$  for two multiwalled nanotubes: S1 ( $d = 27\text{ nm}$ ) and S2 ( $d = 17\text{ nm}$ ). For S1:  $R_{2P}(300\text{ K}) = 5.63\text{ k}\Omega$ , and  $R_{4P}(300\text{ K}) = 2.23\text{ k}\Omega$ , while for S2:  $R_{2P}(300\text{ K}) = 4.5\text{ k}\Omega$  and  $R_{4P}(300\text{ K}) = 2.0\text{ k}\Omega$ . Bottom: The low-temperature resistance is fitted to one-dimensional weak-localization theory.

samples S1 and S2 that upon a  $0.1\text{ eV}$   $E_F$  shift, at least 6 and 4 channels can participate, respectively, in conduction. Indeed, this number of channels can account for most of the resistance measured at  $300\text{ K}$ . Moreover, as in graphite, substitutional boron may also enhance the coupling between the carbon shells of the MWCNT.<sup>13</sup> It is, therefore, possible that more than one shell contributes to conduction even at low bias.

Upon cooling, the B-MWCNT samples in Fig. 1 show an initial linear decrease of both the 2P and 4P resistances down to a crossover temperature  $T^*$ . The linear decrease of the tube resistance with decreasing temperature is characteristic of metals, and has been ascribed to electron-phonon ( $e$ -ph) scattering.<sup>14</sup> While this behavior has been observed in single-walled CNT (SWCNT) bundles,<sup>15,16</sup> to our knowledge it has not been seen in single MWCNT's or SWCNT's. The observation of the metallic behavior in our experiments is due to the reduced influence of the contact resistance in 4P and in 2P measurements, along with the lowering of the Fermi level by the boron doping. The linear slope of the resistance vs temperature curves,  $dR/dT$ , is in the range of  $0.3\text{ }\Omega/\text{K}$  to  $0.5\text{ }\Omega/\text{K}$  in the different B-MWCNT's studied.

The vibrational relaxation time  $\tau_{e-ph}$  can be estimated assuming the tube is a one-dimensional (1D) conductor with a conductance  $G = (2e^2/h)(v_F\tau_{e-ph})N/L$ , where  $v_F$  is the Fermi velocity,<sup>8</sup>  $L$  is the electrode separation, and  $N$  is the number of the participating conduction channels. First, by applying Matthiessen's rule we can extract the elastic mean

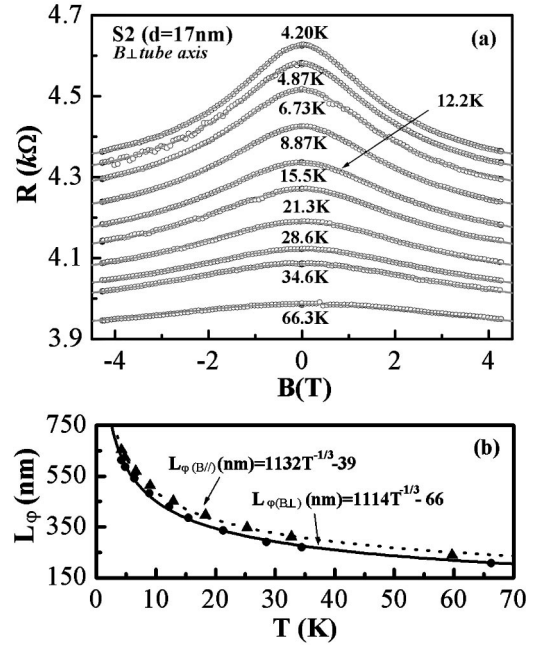


FIG. 2. (a) Two-probe magnetoresistance for S1 at different temperatures in the magnetic field perpendicular to the tube axis, (b) the phase coherence length extracted from the MR in perpendicular field (circles), and parallel field (triangles) as a function of temperature. Lines are the fits to the Nyquist dephasing theory.

free path  $L_{el} = 220\text{--}250\text{ nm}$ , i.e., similar to the spacing between the electrodes. Since the average separation between B atoms is estimated to be below  $10\text{ nm}$ , the large  $L_{el}$  indicates that substitutional boron produces little scattering in MWCNT's. This is in accord with theoretical predictions that point defects in large diameter tubes would lead to very weak back-scattering.<sup>17,18</sup> The relaxation time  $\tau_{e-ph}$  is estimated to be about  $0.4\text{ ps}$  at  $300\text{ K}$ . This value is about 10 times longer than the relaxation time in copper,<sup>19</sup> but about 10 times shorter than a similarly determined relaxation time in undoped SWCNT ropes.<sup>16</sup> The latter is also in agreement with a real time study of energy relaxation in SWCNT ropes.<sup>20</sup> The apparent faster relaxation in B-MWCNT's compared to SWCNT's is likely due to a stronger suppression of back-scattering in the strictly 1D SWCNT's, and the participation of several modes in the B-MWCNT case.

At  $T < T^*$  the resistance starts to increase with decreasing temperature. To determine the origin of this behavior, we first discuss the results of MR measurements over the same temperature range. Figure 2(a) shows the MR of sample S2 measured at different temperatures with the magnetic field perpendicular to the tube axis (circles). A negative MR, i.e., a decrease in  $R$  with increasing field, is observed. Negative MR is characteristic of a material in a WL state due to coherent back-scattering processes.<sup>21,22</sup> This is in accord with the findings of Schonberger *et al.*<sup>23</sup>

The conductance change due to WL for an 1D nanotube with diameter  $D$  and length  $L$  is given by<sup>24,23</sup>

$$\Delta G(B) = \frac{-0.62Ne^2}{\hbar L} \left( \frac{1}{L_\phi^2} + \frac{D^2}{12L_B^2} \right)^{-1/2}, \quad (1)$$

where  $L_\phi$  is the electron phase coherence length, and  $l_B = (h/eB)^{1/2}$  is the magnetic length.  $L_\phi$  is determined by fitting the MR results to Eq. (1). An excellent fit to the experimental data using the 1D-WL theory is shown by the solid lines in Fig. 2(a). (The 2D-WL theory does not give a good fit.) The dominant dephasing mechanism can be determined by analyzing the temperature dependence of  $L_\phi$ . The coherence lengths for S2 at different temperatures are plotted as circles in Fig. 2(b). The fit shows that the  $L_\phi$  between 4 K and 70 K can be described very well by  $L_\phi(nm) = 1114T^{-1/3} - 66$  (solid line). When the magnetic field is parallel to the tube axis, the conductance change is given by<sup>24</sup>

$$\Delta G(B) = \frac{Ne^2}{\pi^2 \hbar L} \left( \frac{1}{L_\phi^2} + \frac{D}{2l_B^2} \right)^{-1/2}. \quad (2)$$

The coherence lengths obtained from the fits of MR in a parallel magnetic field with Eq. (2) are plotted in Fig. 2(b) as triangles. They can be described by  $L_\phi(nm) = 1132T^{-1/3} - 39$  (dashed line). The two measurements of the coherence lengths agree remarkably well with each other over the entire temperature range studied. The temperature dependence of the phase coherence length,  $L_\phi(nm) \propto T^{-1/3}$ , indicates that at low temperatures dephasing is dominated by weakly inelastic electron-electron interactions via the Nyquist mechanism (i.e., interaction of one electron with the fluctuating fields produced by all other electrons) as found in many other 1D and 2D systems.<sup>22,24,25</sup> Completely analogous behavior was observed in sample S1, where the  $L_\phi$  in the range of  $T = 4.2$ –30 K can be expressed as  $L_\phi(nm) = 1861T^{-1/3} - 226$  in the perpendicular field and as  $L_\phi(nm) = 1434T^{-1/3} - 82$  in the parallel field.

Thus, this analysis shows that the coherence lengths are quite long, and that there is an excellent agreement between the data and the predictions of dephasing via Nyquist type scattering over a wide temperature range up to about 70 K. The  $L_\phi$  obtained here are larger than the tube circumference but smaller than the tube length, and also  $L_\phi \gg L_{el}$  at low  $T$ . This indicates that the MWCNT's act as 1D conductors with respect to WL despite their large diameter. Under these conditions the MWCNT's are in the weak-localization regime where transport is diffusive. From the intercept of the  $L_\phi$  vs  $T$  curve, the value of the diffusion coefficient  $D = 0.5 \text{ m}^2 \text{ s}^{-1}$ , and the dephasing time  $\tau \sim 1 \text{ ps}$  (at 4 K) are obtained.

We now return to consider the low-temperature behavior of the resistance (Fig. 1). The theoretical expression for  $R(T)$  due to the first-order quantum correction at  $B = 0$  for a 1D-WL system can be expressed as<sup>24</sup>

$$\frac{R(T) - R_0}{R_0} = \frac{e^2}{\pi^2 \hbar \sigma_u} [6.1L_\phi(T) + 4.91\beta L_T(T)], \quad (3)$$

where  $\sigma_u$  is conductance of the 1D system per unit length,  $\beta$  is a screening factor, and  $L_T = (hD/2\pi k_B T)^{1/2}$  is the thermal length. The temperature dependence of the 2P and 4P resistances for both S1 and S2 tubes can be well described by Eq. (3), as shown by the solid lines in Fig. 1. In the fitting,  $L_\phi(T)$

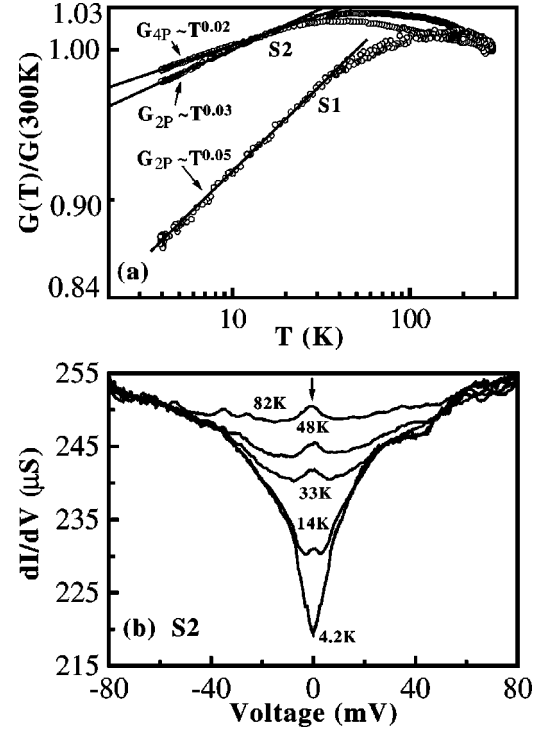


FIG. 3. (a) Temperature dependence of the conductance  $G(T)$  normalized by  $G(300 \text{ K})$  for S1 and S2. (b) Zero-bias anomaly (ZBA) seen in  $dI/dV$  vs  $V$  plots as a function of temperature. The boron-induced peak is indicated by the arrow.

obtained from MR data was used, and it was found that the contribution from the second term in Eq. (3), which describes large energy transfer in  $e$ - $e$  collisions is negligible.

In recent work, the low-temperature dependence of the conductance of SWCNT's has been discussed in terms of Luttinger liquid (LL) theory.<sup>4-6</sup> A key manifestation of the presence of the LL state is the existence of a power-law dependence of the tunneling conductance on temperature:  $G \propto T^\alpha$ . Bockrath *et al.* reported, to the best of our knowledge, for the first time, LL behavior in SWCNT bundles in the range of 8 to 300 K, and obtained values of  $\alpha$  in the range of 0.33 to 0.38 (for bulk coupling of the tube to the leads).<sup>6</sup> More recently, Egger<sup>26</sup> has suggested that the LL state can also be present in MWCNT's. He predicted that the  $\alpha$  exponent of the outer shell would be reduced by the interaction with the other metallic shells in the MWCNT. To test the possibility of a LL-based interpretation of the low-temperature behavior of our B-MWCNT's, we plot the conductance of S1 and S2 as a function of  $T$  on a log-log scale [Fig. 3(b)]. A good power-law fit is obtained at the lowest temperatures, giving  $G(2P)_{S1} \propto T^{0.02}$ , and  $G(4P)_{S1} \propto T^{0.03}$  ( $T$  below  $\sim 30 \text{ K}$ ) and  $G(2P)_{S2} \propto T^{0.05}$  ( $T$  below  $\sim 50 \text{ K}$ ). These measurements are not influenced by Coulomb blockade as in the case of SWCNT's.<sup>6</sup> However, the  $\alpha$  values obtained are very low. Following Egger,<sup>26</sup> these  $\alpha$  values imply screening by an unrealistically large number of metallic shells ( $N > 15$ ) in the MWCNT. Furthermore, Coulomb inhibition of tunneling due to disorder-enhanced correlation also can give rise to a power-law temperature dependence of the conductance.<sup>27</sup>

$dI/dV$  vs  $V$  curves [Fig. 3(b)] show a zero-bias anomaly. Such an anomaly is usually considered as a manifestation of the LL state. However, disorder-enhanced electron correlation can also give rise to a zero-bias anomaly.<sup>28</sup> Finally, we point out a weak peak near  $E_F$  in Fig. 3(b) (see arrow). A similar peak was observed in the STM spectra of B-doped MWCNT's.<sup>12</sup> From the temperature dependence of this peak we can conclude that it originates from the free acceptor  $BC_3$  local structure.

From the above discussion it is clear that although some of our observations are suggestive of the formation of an LL state, all of the observations can be interpreted in terms of coherent back-scattering processes and the formation of a weakly localized state at low temperatures. We note in particular that currently there are no predictions on the behavior of a nanotube in the LL state in a magnetic field.

In conclusion, we have studied the importance of impurity, phonon, and electron-electron scattering on the transport in B-doped MWCNT's. B-doping affects transport by shifting the Fermi level and thus changing the number of participating conduction channels without introducing strong back-scattering. Upon cooling, the resistance of the tubes initially shows a linear decrease with temperature characteristic of

metals. The electron-phonon scattering is weak and leads to only a 2–3 % change in the resistance over the range of 300–4 K. At lower temperatures, the resistance starts to increase. A negative magnetoresistance characterizes this regime indicating the formation of a 1D weakly localized state. The extracted coherence lengths are long, and their temperature dependence indicates that the dominant dephasing mechanism involves electron-electron scattering via a Nyquist mechanism. A comparison of our results with the expectations of the Luttinger liquid and of the coherent back-scattering (weak localization) models shows that only the latter can account for all of the observed low-temperature transport characteristics. The strong influence of boron on the electrical characteristics of the tube, and the similarity of the effects (i.e., electron trapping) produced by boron and by structural defects in graphite, suggest that the puzzling  $p$ -type character of nanotubes may be due, at least in part, to defects and foreign acceptor atoms.

The authors thank B. Ek for expert technical assistance and they gratefully acknowledge P. G. Collins and S. Roche for helpful discussions.

\*Corresponding author. Email address: avouris@us.ibm.com

<sup>1</sup>C. Dekker, Phys. Today **52** (5), 22 (1999).

<sup>2</sup>Teri Wang Odom, Jin-Lin Huang, Philip Kim, and Charles M. Lieber, J. Phys. Chem. B **104**, 2794 (2000).

<sup>3</sup>*Carbon Nanotubes: Synthesis, Structure, Properties, and Applications*, edited by M. Dresselhaus, G. Dresselhaus, and Ph. Avouris (Springer-Verlag, Berlin, 2001).

<sup>4</sup>R. Egger and A.O. Gogolin, Phys. Rev. Lett. **79**, 5082 (1997).

<sup>5</sup>L. Balents and M.P.A. Fisher, Phys. Rev. B **55**, R11 973 (1997).

<sup>6</sup>M. Bockrath, David H. Cobden, J. Lu, A.G. Rinzler, R.E. Smalley, Leon Balent, and Paul L. McEuen, Nature (London) **397**, 598 (1999).

<sup>7</sup>Z. Yao, H.W.Ch. Postma, L. Balents, and C. Dekker, Nature (London) **402**, 6759 (1999).

<sup>8</sup>A. Bachtold, C. Strunk, J.-P. Salvetat, J.-M. Bonard, L. Forro, T. Nussbaumer, and C. Schonenberger, Nature (London) **397**, 673 (1999).

<sup>9</sup>S. Frank, P. Poncharal, Z.L. Wang, and W.A. de Heer, Science **280**, 1744 (1998).

<sup>10</sup>A. Bachtold, M.S. Fuhrer, S. Plyasunov, M. Forero, Erik H. Anderson, A. Zettl, and Paul L. McEuen, Phys. Rev. Lett. **84**, 6082 (2000).

<sup>11</sup>W. K. Hsu *et al.*, Chem. Phys. Lett. **323**, 572 (2000).

<sup>12</sup>D.C. Carrol, Ph. Redlich, X. Blas, J.-C. Charlier, S. Curran, P.M. Ajayan, S. Roth, and M. Ruhle, Phys. Rev. Lett. **81**, 2332 (1998).

<sup>13</sup>C.A. Klein, J. Appl. Phys. **33**, 3338 (1962).

<sup>14</sup>C.L. Kane *et al.*, Europhys. Lett. **41**, 683 (1998).

<sup>15</sup>J.E. Fischer *et al.*, Phys. Rev. B **55**, R4921 (1997).

<sup>16</sup>J. Appenzeller, R. Martel, Ph. Avouris, H. Stahl, and B. Lengeler Appl. Phys. Lett. (to be published).

<sup>17</sup>L. Chico, L.X. Benedict, S.G. Louie, and M.L. Cohen, Phys. Rev. B **54**, 2600 (1996).

<sup>18</sup>C.T. White and T.N. Todorov, Nature (London) **393**, 240 (1998).

<sup>19</sup>R.A. Jishi, M.S. Dresselhaus, and G. Dresselhaus, Phys. Rev. B **48**, 11 385 (1993).

<sup>20</sup>T. Hertel and G. Moos, Phys. Rev. Lett. **84**, 5002 (2000).

<sup>21</sup>A.G. Aronov and Yu.V. Sharvin, Rev. Mod. Phys. **59**, 755 (1987).

<sup>22</sup>B.L. Al'tshuler, A.G. Aronov, M.E. Gershenson, and Yu.V. Sharvin, Sov. Sci. Rev., Sect. A **9**, 223 (1987).

<sup>23</sup>C. Schonenberger, A. Bachtold, C. Strunk, J.-P. Salvetat, and L. Forro, Appl. Phys. A: Solids Surf. **69**, 283 (1999).

<sup>24</sup>B.L. Al'tshuler, A.G. Aronov, and D.E. Khmelnitskii, J. Phys. C **15**, 7367 (1982).

<sup>25</sup>P.M. Echternach *et al.*, Phys. Rev. B **48**, 11 516 (1993).

<sup>26</sup>R. Egger, Phys. Rev. Lett. **83**, 5547 (1999).

<sup>27</sup>S. Levitov and A.V. Shytov, Pis'ma Zh. Éksp. Teor. Fiz. **66**, 200 (1997) [JETP Lett. **66**, 215 (1997)].

<sup>28</sup>B.L. Altshuler, A.G. Aronov, and P. A. Lee, Phys. Rev. Lett. **44**, 1288 (1980).